Synthesis of thermally stable tetragonal zirconia with large surface area and its catalytic activity in the skeletal isomerization of 1-butene

Young-Woong Suh, Jung-Woo Lee, and Hyun-Ku Rhee*

School of Chemical Engineering and Institute of Chemical Processes, Seoul National University, Kwanak-ku, Seoul 151-742, Korea

Received 21 April 2003; accepted 18 July 2003

Thermally stable zirconia with a large BET surface area was prepared by using zirconium atrane derivatives and commercial alkyltrimethylammonium bromide. The zirconia samples were characterized by wide-angle X-ray diffraction, thermal analysis and N_2 adsorption/desorption analysis. The results showed that the present zirconia existed as a thermally stable tetragonal crystallite and consisted of mesoporous material with microporous contribution. The BET surface area was found larger than 240 m^2/g even after calcination at 600 °C. The present zirconia after sulfation was applied to the skeletal isomerization of 1-butene, and its catalytic activity was found superior to that of the conventional sulfated zirconia.

KEY WORDS: tetragonal zirconia; mesoporous material; microporous contribution; large surface area; thermal stability; skeletal isomerization; 1-butene.

1. Introduction

Zirconia has attracted much attention in the areas of ceramics and catalysis. Its catalytic application especially is quite promising because zirconia has both acidic and basic properties [1] and a high thermal stability. In recent years, a number of studies have been reported on the application of zirconia as a catalyst or as a catalyst support [2–4]. More specifically, zirconia was proven active in catalytic reactions including paraffin isomerization [5], CO/CO_2 hydrogenation [6,7], alcohol dehydrogenation [8,9] and hydrogenation of carboxylic acids [10]. Furthermore, sulfate-promoted zirconia has been found to be highly acidic and thus active for the isomerization of lower linear alkanes at low temperatures [11,12].

For an extended application, however, it is required that zirconia must possess large surface area, large pore size, well-developed pore structure and good thermal stability. When compared with other common support materials such as silica and alumina, the commercial zirconia has a rather low surface area of less than 50 m^2/g or even less. Much effort has been attempted to prepare zirconia with a large surface area by using novel preparation methods including the glycothermal process [13], the alcohothermal-SCFD process [14,15] and the CO_2 supercritical drying [16,17] or by incorporating other components such as potassium [18] and rare earth ions [13]. In addition, the surfactant-assisted sol–gel approach has been developed for the purpose of producing mesoporous zirconia with the regular pore structure [19–28]. This approach involves a very elaborate and time-consuming treatment for hydrothermal synthesis and utilizes expensive reagents, but it turns out to be effective in creating materials with large surface areas as well as well-developed pore structure.

As observed with many transition metal oxides, the calcination of zirconium-surfactant composites results in a (partial) structure collapse, except for the material prepared by using PEO-PPO-PEO block copolymers [27]. Therefore, it is very important to achieve an adequate balance between the hydrolysis–condensation process involving zirconium centers and the self-assembling reactions in the surfactant-assisted synthesis of ZrO_2-based mesoporous materials. In practice, it is difficult to form stable mesostructures using transition metal alkoxides because of their high reactivity toward water [29]. Triethanolamine (TEAH) has been recently reported to be a hydrolysis-retarding agent [30–32]. The use of atrane complexes formed by the interaction between metal alkoxides and TEAH allows us to control the hydrolysis and condensation rates of metal alkoxides, and thus ordered mesoporous materials can be synthesized starting from highly reactive metal alkoxides.

On the basis of this synthesis strategy, we have recently reported the preparation of thermally stable mesoporous zirconia using TEAH and commercial alkyltrimethylammonium bromide [33]. It was also demonstrated that the prepared material consists of mesoporous solid with a microporous contribution and a wormhole pore structure. However, the thermal behavior of this material was not systematically investigated.

In the present work, we report the results of physicochemical characterization that provide us with

* To whom correspondence should be addressed.
E-mail: hkrhee@snu.ac.kr

1011-372X/03/0900–0103/0 © 2003 Plenum Publishing Corporation

a new insight into the thermal behavior of the zirconia samples prepared on the basis of the atrane route. The zirconium mesophases were calcined at high temperatures of 350, 500 and 600 °C, respectively, and the resultant materials were characterized by wide-angle XRD, TG/DTA and N_2 adsorption/desorption analyses. In addition, the prepared zirconia was sulfated and then tested for the 1-butene skeletal isomerization, which must be carried out at high reaction temperatures above 350 °C.

2. Experimental

2.1. Sample preparation

Zirconium atrane (Zr-atrane) derivatives were prepared by using zirconium *n*-propoxide and TEAH in tetrahydrofuran (THF) according to the synthetic method of titanatranes described in the literature [34,35]. In a typical synthesis leading to the zirconia mesophase, NaOH was dissolved at 60 °C in a TEAH solution containing the prepared Zr-atrane derivatives and the surfactant, cetyltrimethylammonium bromide (CTAB) or octadecyltrimethylammonium bromide (OTAB) and then water was slowly added under vigorous stirring at 120 °C. Thus, the molar composition of the starting reagent mixture was: 2 Zr-atrane : 7.5 TEAH : 0.7 NaOH : 0.6 surfactant: $\sim 332 H_2O$. The resulting mixture was stirred for 2 h and then allowed to cool down to room temperature to realize the formation of a pale yellow solid. This was hydrothermally aged at 120 °C for 2 days. After aging, the solid was filtered off, washed with ethanol and air-dried. Finally, the surfactant was removed by calcination at 350 °C for 120 h according to the method of Cabrera *et al.* [31]. In addition, the material was calcined at high temperatures of 500 and 600 °C, respectively, under air atmosphere for 6 h.

Sulfate promotion was carried out by immersing 0.15 g of the zirconia sample in 10 mL of 3 M H_2SO_4 solution for 90 min. The sample was filtered off and dried at 100 °C overnight. It was then kept in a vacuum desiccator to prevent any contamination of the catalyst prepared.

2.2. Characterization

Powder X-ray diffraction patterns in the 2θ range of 1–10° were collected at ambient temperature using Cu Kα radiation, $\lambda = 1.54056$ Å, on a Philips X'Pert MPD diffractometer operating at 40 kV and 40 mA. Simultaneous thermogravimetric (TG) and differential thermal analysis (DTA) measurements were performed on a TA Instruments SDT-2960 thermal analyzer apparatus in air flow (100 mL/min) with a heating rate of 10 K/min. Nitrogen adsorption and desorption isotherms were measured at 77 K using a Micromeritics 2010 system after the samples were first degassed at 200 °C overnight. Surface areas (S_{BET}) were determined by the BET method in the 0.05–0.1 relative partial pressure range, and the pore size distribution in the adsorption branch of the isotherm was determined by the Barrett–Joyner–Halenda (BJH) method. The total pore volume (V_t) was taken at the $P/P_0 = 0.99$ single point and the micropore volume (V_{mi}) was calculated by using Horvath–Kawazoe formula in the diameter range of < 20 Å.

2.3. Catalytic tests

The skeletal isomerization of 1-butene was carried out in gas phase in a fixed-bed flow reactor at atmospheric pressure. The catalyst (0.1 g) was loaded into the reactor and pretreated at 500 °C before the reaction. After pretreatment, the reactor was cooled down to the reaction temperature of 450 °C; and then, 1-butene in He balance (the ratio of He to 1-butene =9 : 1) was streamed into the reactor at a flow rate of 10 mL/min. The samples were taken out periodically during the course of reaction with Valco 16-port multiposition valve and analyzed by an on-line gas chromatography (HP5890) equipped with HP-PLOT/Al_2O_3 capillary column and FID. The conversion was calculated in terms of mole-percent of 1-butene consumed and the selectivity to isobutene in terms of the yield of isobutene divided by the conversion of 1-butene. 2-butenes were not considered as products because the isomerization between 1-butene and 2-butene is much faster than the skeletal isomerization, and 2-butenes can also be converted into isobutene [36,37].

3. Results and discussion

3.1. Characterization of mesoporous zirconia prepared on the basis of the atrane route

The XRD patterns of the calcined zirconia samples synthesized in this study are shown in figure 1. Figure 1(a) displays the XRD patterns recorded for the zirconia prepared by using CTAB as the surfactant and subsequently calcined at different temperatures of 350, 500 and 600 °C, respectively. After calcination at 350 °C, the broad diffraction pattern was observed, indicating a characteristic of tetragonal zirconia nanoparticles with a low crystallinity.

Table 1 presents the mean crystalline sizes (D_{hkl}) of the zirconia samples, deduced from the full width at half-maximum for the (1 1 1) reflection of the tetragonal phase using the Scherrer relationship. The mean crystalline size for the zirconia calcined at 350 °C was measured to be about 1.0 nm. As the calcination temperature increases, the diffraction peaks tend to sharpen, and this suggests a further enlargement of the crystallite size up

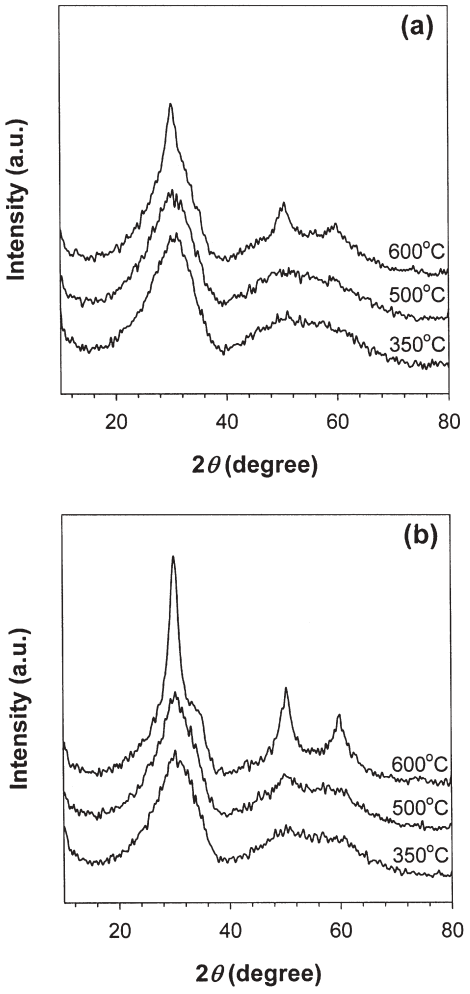

Figure 1. XRD patterns of the zirconia samples synthesized with the surfactant, (a) CTAB or (b) OTAB, and subsequently calcined at different temperatures of 350, 500 and 600 °C.

to 1.4 nm. However, the calcination at higher temperatures did not change the XRD pattern phase of the zirconia except for the peaks' becoming sharper and stronger. This indicates that the calcination does not lead to the transformation of the tetragonal to monoclinic phase of zirconia.

On the other hand, no basic difference was observed between the XRD patterns for the two zirconia samples prepared by using CTAB and OTAB surfactants, respectively (see figure 1(a) and (b)). After calcination at 600 °C for 6 h, however, the diffraction peaks for the zirconia synthesized with OTAB surfactant were observed to be sharper than those for the zirconia synthesized with CTAB surfactant, suggesting that the former had a larger tetragonal crystallite with a size of about 2.3 nm than the latter (table 1). The reason for this will be discussed below.

Figure 2 shows the results of thermal analyses for the zirconia mesophases prepared with CTAB and OTAB surfactants, respectively. In the upper diagram, we observe two weight losses, one at 70 °C and the other at around 330 °C. The former can be attributed to the loss of physically adsorbed water. On the other hand, the latter loss completed below 500 °C was highly exothermic, originating from the combustion of surfactants. However, the present TG weight loss curve is quite different from the result observed in a hydrous zirconia gel obtained by the conventional method [38].

In general, zirconia always exhibits a strong exothermal response easily observed by DTA analysis, which results from the crystallization of zirconia or the transformation of tetragonal to monoclinic phase. Inoue *et al.* [39] also reported that the surface area rapidly decreased with a further increase in the calcination temperature (> 500 °C) due to the modification of zirconia. However, the DTA data for the present zirconia mesophases show no distinct endotherms or exotherms/glow exotherms, indicating that the substantial transition of an amorphous phase into crystalline zirconia or the significant transformation of $t \rightarrow m$ phase did not take place. This is in good agreement with the results obtained by the XRD analysis. According to the conclusion suggested by Garvie and coworkers [40,41], the tetragonal phase is stable below the

Table 1
Physicochemical properties of zirconia samples calcined at different temperatures[a]

Surfactant	T_{calc} [b] (°C)	d_{100} [c] (nm)	S_{BET} (m^2/g)	V_t (cm^3/g)	V_{mi} (cm^3/g)	D_p [d] (nm)	t [e] (nm)	D_{hkl} (nm)
CTAB	350	4.7	406	0.41	0.19	2.1	2.6	1.0
	500	4.4	330	0.33	0.15	2.0	2.4	1.1
	600	4.1	243	0.24	0.11	1.8	2.3	1.4
OTAB	350	5.0	361	0.38	0.16	2.5	2.5	1.0
	500	4.7	358	0.37	0.16	2.4	2.3	1.1
	600	4.3	284	0.27	0.12	2.0	2.3	2.3

[a] Zirconia samples were prepared by using CTAB or OTAB as a surfactant.
[b] Calcination temperature.
[c] d (100) spacing.
[d] The pore diameter (D_p) was determined from the maximum point of BJH pore size distribution plot obtained from the adsorption branch of the isotherm.
[e] The wall thickness (t) was calculated by simple subtraction of pore diameter (D_p) from d_{100} value.

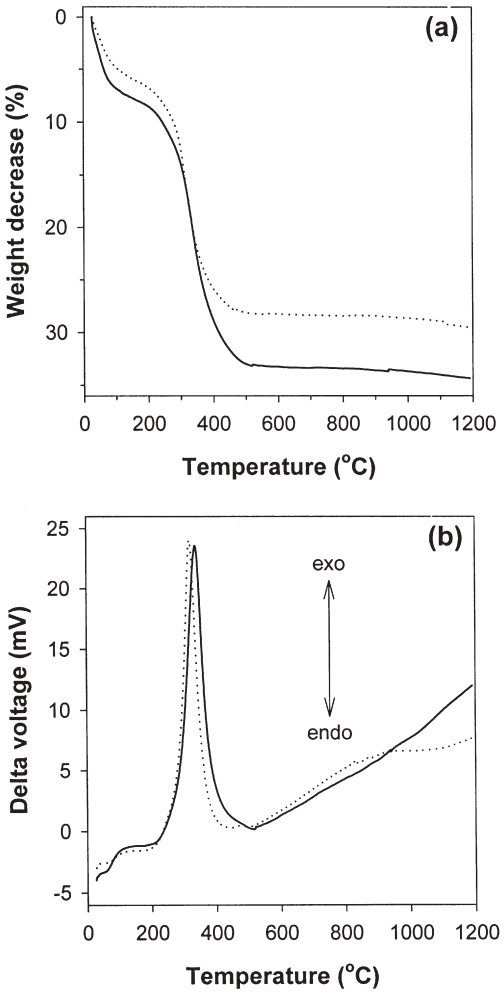

Figure 2. Thermal analysis profiles of the zirconia mesophases prepared with the surfactant, CTAB (solid line) or OTAB (dotted line): (a) TG and (b) DTA.

transformation temperature (i.e., 1174 °C) when the crystallite size is smaller than the critical value of about 10–15 nm because of the surface and strain energy effect. This argument then clearly explains why the present zirconia samples could exist in a thermally stable tetragonal phase.

Two different features are observed between the TG/DTA curves for the zirconia mesophases prepared by using CTAB and OTAB surfactants, respectively; one is in regard to the total weight loss and the other is in regard to the peak temperature (T_{peak}) taken from the peak point of the exothermic curve in the DTA measurement. Since the total weight loss is related to several substances including the contaminants on the surface of the sample, the coordinated water or hydroxyl group and the surfactant, it would be difficult to discuss clearly the difference in the total weight loss between the two materials. However, the zirconia mesophase synthesized with OTAB surfactant showed an exothermal transition at a lower temperature ($T_{peak} = 318$ °C) than the one synthesized with CTAB surfactant ($T_{peak} = 336$ °C). This means that the former undergoes the crystallization of an amorphous phase earlier than the latter. The DTA data thus confirm the XRD results, i.e., after calcination at 600 °C for 6 h, the zirconia synthesized with OTAB surfactant had a larger tetragonal crystallite than the one synthesized with CTAB surfactant. This feature is supported by the results of Stichert and Schüth [38].

The nitrogen adsorption/desorption isotherms of zirconia samples are shown in figure 3(a). The overall shapes of all the isotherms are similar, regardless of the type of surfactant used and irrespective of the conditions under which the sample was calcined. All the zirconia samples exhibited isotherms of an intermediate mode between type IV, characteristic of mesoporous materials, and type I, which is related to microporous materials. This indicates that the prepared zirconia samples are mesoporous with microporous contribution, although hysteresis loops are evident. The microporosity observed in this study may be associated with the characteristic feature of the organic compound

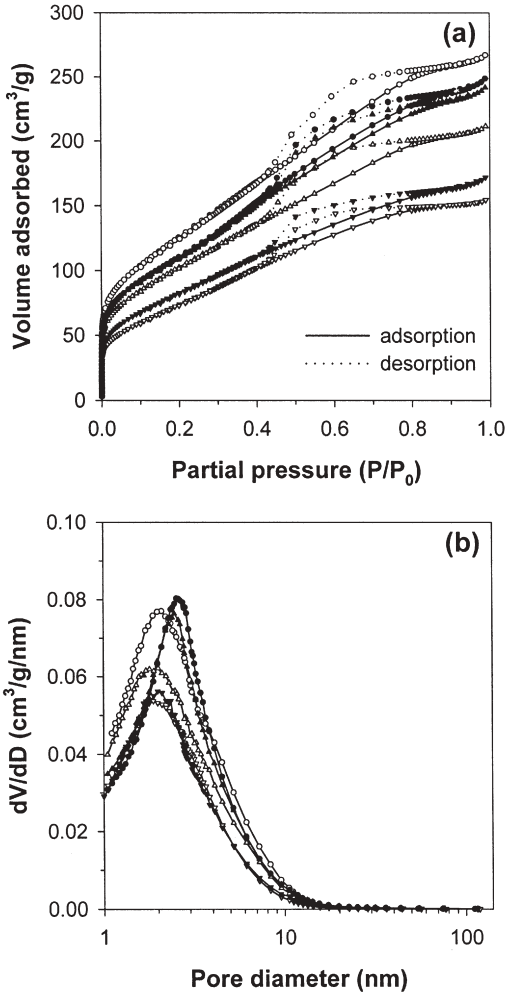

Figure 3. (a) N_2 adsorption/desorption isotherms and (b) BJH pore size distribution plots calculated from the adsorption branches of the isotherms for the zirconia samples synthesized with the surfactant, CTAB (open key) or OTAB (filled key), and subsequently calcined at 350 °C (○, ●), 500 °C (△, ▲) and 600 °C (▽, ▼).

TEAH because TEAH can act as a micropore-forming agent [42,43]. Figure 3(b) presents the pore size distributions calculated by the BJH method. All of the zirconia samples exhibited no narrow pore size distributions. Such a characteristic may be considered to be unique if one examines those reported for zirconium oxides with large surface areas that were prepared by various methods without surfactants [15–17,44]. Those materials were observed to exhibit a textural mesoporosity of larger than 10 nm, whereas the present zirconia had a framework-confined wormhole pore structure in the range of 2–10 nm.

The physicochemical properties of zirconia samples synthesized with commercial alkyltrimethylammonium bromide are summarized in table 1. As the calcination temperature increases, all the properties tend to decrease in both zirconia samples except for the mean crystalline size. Such a decrease is a general feature originating from the pore shrinkage. However, the extent of decrease is smaller in the sample synthesized with OTAB surfactant because of the longer length of hydrophobic tail in the OTAB surfactant [33].

It is worth noting that the present zirconia samples maintain rather large surface areas, larger than 240 m^2/g, even after calcination at a high temperature of 600 °C. It is evident that the present zirconia has a BET surface area larger than any other zirconia material prepared without surfactant by employing several methods such as the alcohothermal-SCFD process [14,15] and the CO_2 supercritical drying [16,17]. Therefore, the atrane route enables us to prepare a thermally stable tetragonal zirconia with a large surface area. It is expected that the zirconia synthesized by using the present atrane route may have a good potential for application to catalytic reactions, especially to acid-catalyzed reactions, after sulfation.

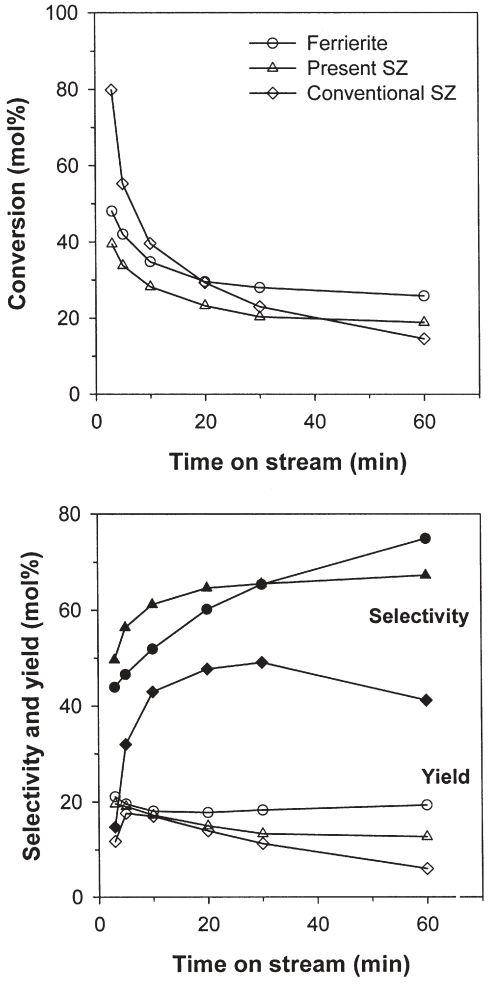

Figure 4. Conversion of 1-butene, selectivity to isobutene and yield of isobutene obtained at 450 °C over Ferrierite, the present sulfated zirconia (SZ) and the conventional SZ.

3.2. *Catalytic activity in the skeletal isomerization of 1-butene*

The present zirconia was applied after sulfation to the 1-butene skeletal isomerization at a reaction temperature of 450 °C. Figure 4 shows the catalytic activities obtained over Ferrierite, the conventional sulfated zirconia (SZ) and the present SZ. The conventional SZ deactivated very rapidly. The selectivity to isobutene increased until the reaction time of 30 min, but decreased afterwards. The present SZ was found to deactivate at a rate lower than the conventional SZ. Also, the higher and more stable selectivity to isobutene was observed with the present SZ than with the conventional SZ.

A large number of acid catalysts have been reported to show a high isobutene selectivity in the skeletal isomerization of 1-butene; e.g. Ferrierite [36,45–48], MCM-22 [37], aluminophosphate [49,50], fluorinated alumina [51–54] and tungsten oxide supported on alumina [55]. Among them, medium-pore zeolite Ferrierite (FER topology) is known to be very active for this reaction with an exceptional selectivity to isobutene [36,45–48]. The FER structure, which contains a two-dimensional pore system consisting of ten-membered rings (4.2 × 5.4 Å) intersected by eight-membered rings (3.5 × 4.8 Å), was reported to play a central role in achieving such a high selectivity to isobutene [36,45–48]. In view of the isobutene selectivity, the present SZ is comparable to Ferrierite. Such a remarkable reaction result with the present SZ may be attributed to its peculiar pore structure, i.e., a mesoporous material with microporous contribution. When micropore size distribution plot was calculated by using the Horvath-Kawazoe method in the diameter range of < 20 Å, a very sharp peak centered at a pore diameter of ca. 5.1 Å was observed in all the zirconia samples. This pore diameter is found to be nearly the same as that of FER zeolite. Therefore, one may explain why the present SZ shows such an excellent selectivity to isobutene as follows: the reactant, which can enter readily into the

mesopores of the present SZ catalyst, may be converted selectively to the desired product isobutene inside the micropores whose diameter is similar to that of FER zeolite.

Table 2 presents the conversion of 1-butene and the product yields obtained over the present SZ catalysts with 1-butene space velocity (WHSV) of 4.51 h^{-1}, 1-butene partial pressure of 0.1 atm and time on stream of 30 min. Besides isobutene, C_2 to C_6 saturated and unsaturated hydrocarbons were produced during the reaction by undesired secondary reactions such as dimerization, oligomerization, cracking and hydrogen transfer, leading to the formation of by-products [37,45–55]. Among these, isobutane, propylene and pentenes were the major by-products formed over the present SZ catalysts. Especially, propylene and pentenes are well known to be produced through the dimerization-cracking process [37,45]. Hydrocarbons higher than C_6 were not observed in the reaction products.

As the calcination temperature increased, 1-butene conversion as well as all the product yields decreased as may be noticed in table 2. The decrease is related to the BET surface area. If all the catalysts are treated by the same amount of sulfate, the acid site density decreases with the increase in the surface area and, thus, the acid sites would become more isolated [37]. Isobutene can be formed by monomolecular process and bimolecular dimerization(oligomerization)-cracking processes [37,45]. In case of MCM-22, the isobutene yield remains at the same level, regardless of the zeolite Si/Al ratio, and this indicates that isobutene is mainly formed via direct isomerization of 1-butene because monomolecular process would be much less affected than bimolecular ones by the change in the acid site density of the zeolite [37]. Therefore, it is understood that the change in the acid site density affects the latter more strongly than the former in the case of our present SZ catalyst. On the basis of this argument, one can claim that isobutene is mainly formed by bimolecular processes on the present catalyst. This is also supported by the results that there is not much difference in the 1-butene conversion and the product yields obtained on the SZ catalysts synthesized with OTAB surfactant and subsequently calcined at 350 and 500 °C, respectively, and that the two materials have similar BET surface areas (see table 1).

4. Conclusions

Thermally stable tetragonal zirconia with a large surface area has been prepared on the basis of the atrane route, which utilizes commercial alkyltrimethylammonium bromide and zirconium atrane derivatives. The results of XRD and TG/DTA analyses revealed that this material consisted of only the tetragonal crystallite with a size in the range 1–2.4 nm. It was shown by N_2 adsorption/desorption analysis that the present zirconia is a mesoporous material with microporous contribution and framework-confined wormhole pore structure. It is also worth noting that the present zirconia maintains a rather large surface area, which is larger than 240 m^2/g even after calcination at a high temperature of 600 °C. When applied to the skeletal isomerization of 1-butene, the present zirconia after sulfation was found to show a higher and more stable selectivity to isobutene compared to the conventional SZ. This is attributed to the peculiar pore structure of the present zirconia. Furthermore, the reaction result suggests that isobutene is produced on the present SZ through bimolecular processes. Consequently, it is evident that the zirconia prepared in this study has a good potential for catalytic application.

Acknowledgments

The authors gratefully acknowledge the financial support of the LG-Caltex Oil Corporation and the partial aid from the Brain Korea 21 Program, sponsored

Table 2
Conversion of 1-butene and product yields obtained in the skeletal isomerization of 1-butene over the sulfated zirconia catalysts [a]

Surfactant used	T_{calc} [b] (°C)	Conversion (mol%)	Yield (mol%) [c]						
			$C_2^=$	$C_3^=$	C_4 [d]	i-$C_4^=$	C_5 [d]	$C_5^=$	$C_6^=$
CTAB	350	42.3	0.4	7.2	10.1	18.3	1.2	4.8	0.0
	500	37.5	0.2	6.7	7.9	16.8	1.1	4.7	0.0
	600	18.7	0.1	2.8	1.8	11.6	0.2	2.3	0.0
OTAB	350	39.3	0.3	6.6	9.6	16.7	1.2	4.6	0.1
	500	36.2	0.3	6.3	8.0	15.9	1.1	4.4	0.1

[a] Zirconia samples were synthesized with the surfactant, CTAB and OTAB, respectively, and subsequently calcined at different temperatures of 350, 500 and 600 °C, respectively.
[b] Calcination temperature.
[c] Reaction conditions: 450 °C, 0.1 atm of 1-butene, 4.51 h^{-1} WHSV, 30 min TOS.
[d] C_4 = isobutane + n-butane, C_5 = isopentane + n-pentane.

by the Ministry of Education. We are also indebted to Dr. Chae-Ho Shin for the BET analysis.

References

[1] K. Tanabe, Mater. Chem. Phys. 13 (1985) 347.
[2] T. Yamaguchi, Catal. Today 20 (1994) 199.
[3] K. Tanabe and T. Yamaguchi, Catal. Today 20 (1994) 185.
[4] B.H. Davis, R.A. Keogh and R. Srinivasan, Catal. Today 20 (1994) 219.
[5] Y. Nakano, T. Lizuka, H. Hattori and K. Tanabe, J. Catal. 57 (1979) 1.
[6] Y. Amenomiya, Appl. Catal. 30 (1987) 57.
[7] Y.W. Suh, S.H. Moon and H.K. Rhee, Catal. Today 63 (2000) 447.
[8] T. Yamaguchi, H. Sasaki and K. Tanabe, Chem. Lett. (1973) 1017.
[9] B.H. Davis and P. Ganesan, Ind. Eng. Chem. Prod. Res. Dev. 18 (1979) 191.
[10] T. Yokoyama, T. Setoyama, N. Fujita, M. Nakajima, T. Maki and K. Fujii, Appl. Catal. 88 (1992) 149.
[11] M. Hino, S. Kobayashi and K. Arata, J. Am. Chem. Soc. 101 (1979) 6439.
[12] T. Yamaguchi, Appl. Catal. 61 (1990) 1.
[13] M. Inoue, K. Sato, T. Nakamura and T. Inui, Catal. Lett. 65 (2000) 79.
[14] J.C. Hu, Y. Cao and J.F. Deng, Chem. Lett. (2001) 398.
[15] Y. Cao, J.C. Hu, Z.S. Hong, J.F. Deng and K.N. Fan, Catal. Lett. 81 (2002) 107.
[16] D.A. Ward and E.I. Ko, Chem. Mater. 5 (1993) 956.
[17] D.J. Suh and T.J. Park, Chem. Mater. 14 (2002) 1452.
[18] G.K. Chuan and S. Jaenicke, Appl. Catal., A 163 (1997) 261.
[19] U. Ciesla, S. Schacht, G.D. Stucky, K.K. Unger and F. Schüth, Angew. Chem. Int. Ed. Engl. 35 (1996) 541.
[20] J.S. Reddy and A. Sayari, Catal. Lett. 38 (1996) 219.
[21] J.A. Knowles and M.J. Hudson, J. Chem. Soc. Chem. Commun. (1995) 2083.
[22] J.L. Blin, R. Flamant and B.L. Su, Inter. J. Inorg. Mater. 3 (2001) 959.
[23] G. Pacheco, E. Zhao, A. Garcia, A. Sklyarov and J.J. Fripiat, Chem. Commun. (1997) 491.
[24] M.S. Wong and J.Y. Ying, Chem. Mater. 10 (1998) 2067.
[25] G. Larsen, E. Lotero, M. Nabity, L.M. Petkovic and D.S. Shobe, J. Catal. 164 (1996) 246.
[26] Y.Y. Huang, T.J. McCarthy and W.M.H. Sachtler, Appl. Catal., A 148 (1996) 135.
[27] P. Yang, D. Zhao, D.I. Margolese, B.F. Chmelka and G.D. Stucky, Nature 396 (1998) 152.
[28] X. Yang, F.C. Jentoft, R.E. Jentoft, F. Girgsdies and T. Ressler, Catal. Lett. 81 (2002) 25.
[29] J. Livage, M. Henry and C. Sachez, Prog. Solid State Chem. 18 (1988) 259.
[30] S. Cabrera, J. El Haskouri, J. Alamo, A. Beltrán, D. Beltrán, S. Mendioroz, M.D. Marcos and P. Amorós, Adv. Mater. 11 (1999) 379.
[31] S. Cabrera, J. El Haskouri, A. Beltrán-Porter, D. Beltrán-Porter, M.D. Marcos and P. Amorós, Solid State Sci. 2 (2000) 513.
[32] S. Cabrera, J. El Haskouri, C. Guillem, J. Latorre, A. Beltrán-Porter, D. Beltrán-Porter, M.D. Marcos and P. Amorós, Solid State Sci. 2 (2000) 405.
[33] Y.-W. Suh, J.-W. Lee and H.-K. Rhee, Solid State Sci., in press (2003).
[34] W.M.P.B. Menge and J.G. Verkade, Inorg. Chem. 30 (1991) 4628.
[35] A.A. Naiini, S.L. Ringrose, Y. Su, R.A. Jacobsen and J.G. Verkade, Inorg. Chem. 32 (1993) 1290.
[36] G. Seo, H.S. Jeong, S.B. Hong and Y.S. Uh, Catal. Lett. 36 (1996) 249.
[37] M.A. Asensi, A. Corma and A. Martínez, J. Catal. 158 (1996) 561.
[38] W. Stichert and F. Schüth, Chem. Mater. 10 (1998) 2020.
[39] M. Inoue, H. Kominami and T. Inui, Appl. Catal. 97 (1993) L25.
[40] R.C. Garvie, J. Phys. Chem. 82 (1978) 218.
[41] R.C. Garvie and M.F. Goss, J. Mater. Sci. 21 (1986) 1253.
[42] Z. Shan, T. Maschmeyer and J.C. Jansen, Delft University of Technology, ABB Lummus Global Inc., WO 00/15551 (2000).
[43] Z. Shan, E. Gianotti, J.C. Jansen, J.A. Peters, L. Marchese and T. Maschmeyer, Chem. Eur. J. 7 (2001) 1437.
[44] P.D.L. Mercera, J.G. van Ommen, E.B.M. Doesburg, A.J. Burggraaf and J.R.H. Ross, Appl. Catal. 57 (1990) 127.
[45] M. Guisnet, P. Andy, N.S. Gnep, E. Benazzi and C. Travers, J. Catal. 158 (1996) 551.
[46] Z.R. Finelli, C.A. Querini, N.S. Fígoli and R.A. Comelli, Appl. Catal., A 187 (1999) 115.
[47] H.H. Mooiweer, K.P. de Jong, B. Kraushar-Czarnetzki, W.H.J. Stork and B.C.H. Krutzen, Stud. Surf. Sci. Catal. 84 (1994) 2327.
[48] G. Seo, S.H. Park and J.H. Kim, Catal. Today 44 (1998) 215.
[49] S.M. Yang, H.D. Guo, J.S. Lin and G.T. Wang, Stud. Surf. Sci. Catal. 84 (1994) 1677.
[50] L.H. Gielgens, I.H.E. Veenstra, V. Ponec, M.J. Haanepen and J.H.C. van Hooff, Catal. Lett. 32 (1995) 195.
[51] J. Szabo, J. Perrotey, G. Szabo, J.C. Duchet and D. Cornet, J. Mol. Catal. 67 (1991) 79.
[52] Z.X. Cheng and V. Ponec, J. Catal. 148 (1994) 607.
[53] Z.X. Cheng and V. Ponec, Appl. Catal. 118 (199) 127.
[54] G. Seo, N.H. Kim, Y.H. Lee and J.H. Kim, Catal. Lett. 51 (1998) 101.
[55] L.H. Gielgens, M.G.H. van Kampen, M.M. Broek, R. van Hardeveld and V. Ponec, J. Catal. 154 (1995) 201.